Quasifission in ^{84,86}Kr-induced reactions populating superheavy elements

A. Sen [1,2] T. K. Ghosh [1,2,*] E. M. Kozulin [3] I. M. Itkis [3] G. N. Knyazheva [3] K. V. Novikov [3] S. Bhattacharya,[1,†]
K. Banerjee [1,2] and C. Bhattacharya[1,2]

[1]*Variable Energy Cyclotron Centre, 1/AF Bidhan Nagar, Kolkata 700064, India*
[2]*Homi Bhabha National Institute, Anushakti Nagar, Mumbai 400094, India*
[3]*Flerov Laboratory of Nuclear Reactions, Joint Institute for Nuclear Research, 141980 Dubna, Russia*

Background: Quasifission plays a detrimental role in the synthesis of superheavy elements. Understanding the dynamics of quasifission helps in selecting the optimum target projectile combinations for the synthesis of new superheavy elements.

Purpose: The influence of various entrance channel parameters on the quasifission dynamics was explored. Three reactions, ^{84}Kr + ^{198}Pt, ^{86}Kr + ^{198}Pt, and ^{86}Kr + ^{197}Au, expected to be dominated by quasifission, were studied near the Coulomb barrier energies.

Methods: The binary fission fragments from the three reactions were detected using the double arm time-of-flight spectrometer CORSET. The mass and total kinetic energy distributions, which are sensitive to the quasifission dynamics, were measured and analyzed for the three reactions.

Results: The mass and total kinetic energy distributions of all the three reactions have the characteristics that show the dominance of quasifission. For the reaction ^{84}Kr + ^{198}Pt, symmetric quasifission has been found to be relatively more dominant compared to ^{86}Kr + ^{198}Pt reaction. The results have been compared with ^{48}Ca- and ^{52}Cr-induced reactions, populating nearby nuclei, to understand the evolution of quasifission. An analysis of the timescales in these reactions using a dynamical calculation shows that ^{84}Kr + ^{198}Pt takes a longer time to reach a particular dinuclear shape compared to the other two reactions. The driving potential at the barrier radius also shows a shallower pocket for ^{84}Kr + ^{198}Pt compared to ^{86}Kr + ^{198}Pt and ^{86}Kr + ^{197}Au reactions.

Conclusion: The entrance channel isospin difference is found to influence the quasifission dynamics. A higher entrance channel isospin difference may have a larger evolution time, thus driving the systems toward a more symmetric mass split.

I. INTRODUCTION

Synthesis of superheavy elements (SHE) in the laboratory [1–4] requires fusion of two heavy nuclei. The fusing nuclei must have enough kinetic energy to overcome the repulsive electrostatic energy to come within the range of the attractive nuclear forces and fuse to form a compound nucleus (CN). However, the evolution of the fusion path is governed by the complicated multidimensional potential energy landscape [5] which depends critically on the entrance channel parameters (e.g., deformation of target/projectile, mass asymmetry, charge product of target and projectile, collision energy, etc.). The colliding system, after crossing the fusion barrier forms an incompletely equilibrated composite which may gradually evolve either to become a fully equilibrated CN or to escape the barrier before complete equilibration and split into two fragments (known as quasifission [6]). The CN, if formed, either cools down through particle evaporation to form an evaporation residue or undergoes shape oscillations

over the unconditional saddle point, leading to compound nuclear fission (CNF) [7]. The characteristics of CNF is, however, different from the quasifission as the degrees for which equilibration is achieved in the two cases are different. Different experimental probes, e.g., mass, angle, mass-total kinetic energy distributions, mass-angle distributions of the fission fragments, etc., that are sensitive to the degrees of equilibration, are used to differentiate the two processes [8–11].

It is evident that by the presence of the quasifission process, the subsequent probability of synthesis of SHE is adversely affected, as it critically depends on the CN formation. Therefore, for an optimum choice of projectile-target combination for the synthesis of new SHE, a proper understanding of the phenomenon of quasifission is very important. Theoretically, it is difficult to predict the quasifission evolutionary path of any system precisely, as the topography of the potential energy surface is far too complicated. Besides, the dynamical approach proposed by Zagrebaev and Greiner [7] suggests a significant overlap of fusion-fission and quasifission [12]. So it is of foremost importance to use different experimental probes together with the phenomenological understandings and microscopic calculations [13–16] to explore various facets of the formation mechanism of SHE.

*tilak@vecc.gov.in
†Superannuated

TABLE I. The entrance channel properties of the reactions: $Z_p Z_t$ is the charge product; χ_M is the mean fissility parameter [12]; α_0 is the entrance channel mass asymmetry $= (A_t - A_p)/(A_t + A_p)$, where A_t, A_p are the target and projectile mass numbers, respectively; and β_2 is the static deformation parameter [29].

Reaction	System	$Z_p Z_t$	χ_M	α_0	β_2^{proj}	β_2^{target}
^{84}Kr $+$ ^{198}Pt	^{282}Fl	2808	0.922	0.404	0.086	-0.115
^{86}Kr $+$ ^{198}Pt	^{284}Fl	2808	0.917	0.394	0.000	-0.115
^{86}Kr $+$ ^{197}Au	^{283}Mc	2844	0.925	0.392	0.000	-0.125

The seminal experimental works by Toke *et al.* [17] and Shen *et al.* [18] indicated that the fusion of two massive nuclei at energies around the Coulomb barrier is significantly different compared to that for light projectile–induced reaction. This is due to the difference of the Coulomb repulsion between the interacting heavy nuclei as well as the dissipative dynamics that comes into play. Quasifission evolves with the charge product of the projectile-target combination ($Z_p Z_t$) and is the relatively dominant process in nuclear reactions with $Z_p Z_t \geqslant 1600$ (where Z_p and Z_t are the atomic numbers of the projectile and target nuclei, respectively), directly competing with the process of fusion-fission [19]. Although the inhibition of fusion and thereby, the presence of quasifission had also been reported [20] for systems with $Z_p Z_t$ much lower than 1600, those could not be established from the measurement of angular distributions [21]. However, the reactions with very high $Z_p Z_t$, such as the ones studied in this work, are dominated by the quasifission process.

Several experimental probes are known to be sensitive to the presence or absence of quasifission in a nuclear reaction. As the mass degree of freedom in the quasifission process is not equilibrated, an anomalous increase in the width of the mass distribution [22,23] of the fission fragments is one of the signatures of quasifission. Another widely studied probe is the mass-angle correlation [24], where the correlation arises between the fission fragment mass and its angle of emission, due to incomplete equilibration in mass and shape of the dinucleus. Full dissipation of total kinetic energy is not achieved in this process; the width and the peak of the total kinetic energy (TKE) distribution provide a clear indication of the presence of the quasifission process [25–28]. In addition, mass-total kinetic energy (M-TKE) correlation also provides information of symmetric or asymmetric quasifission, where the fragment masses peak around either half of the CN mass or target/projectile masses, respectively [12].

The aim of the present experimental study is a continuation of our endeavour [26,27] to systematically understand the role of quasifission in the reactions relevant to the production of superheavy elements. The entrance channel properties of the reactions under study were chosen so that the mean fissility (χ_M) and static deformations (β_2) of the target projectile combinations are very close to each other, as listed in Table I. Since the above parameters, known to strongly influence the quasifission dynamics [8,30], are nearly the same for the present systems, the influence of other parameters like isospin can be disentangled. The mass and energy distributions of fission like fragments formed in the reactions ^{84}Kr $+$ ^{198}Pt and ^{86}Kr $+$ ^{198}Pt populating two isotopes of the superheavy element flerovium ($Z = 114$) near

the Coulomb barrier energy have been measured to explore the role of the different number of neutrons in the projectile with same $Z_p Z_t$ (=2808) in the entrance channel. The results have also been compared with a more mass asymmetric reaction ^{52}Cr $+$ ^{232}Th that produces a similar compound nucleus ($Z = 114$). To expound the systematic trend of QF in the mass symmetric reactions, the M-TKE distributions of fission like fragments formed in ^{86}Kr $+$ ^{197}Au reaction, populating moscovium ($Z = 115$), at energies above the Coulomb barrier, have also been measured.

II. EXPERIMENTAL DETAILS

The experiments were carried out at the U400M cyclotron facility at Flerov Laboratory of Nuclear Reactions, JINR, Dubna, Russia. The fission fragment masses and kinetic energies were measured using the CORSET spectrometer [31], which consists of two arms, each with an multi channel plate (MCP)-based start detector and a position-sensitive MCP-based stop detector. In each arm, the start and stop detectors were placed 5 and 27 cm away from the target center, respectively. The arms were rotated to collect the data in the angular range of 30° to 68°. The time-of-flight between the start and the stop detectors, the polar and azimuthal positions of each event were measured using the spectrometer. Targets of thickness $\sim$200 μg/cm^2 of enriched ^{198}Pt (99.99%) on titanium backing ($\sim$1.3 μm) and self-supporting ^{197}Au of thickness $\sim$200 μg/cm^2 were used in the experiments. The backing of the ^{198}Pt target was made to face the beam. The energy loss due to the target backing was taken into account during the analysis. Energy losses of the fragments in half of the target thickness and the conversion foils of the start detectors were corrected on an event-by-event basis. The fission fragment mass distributions were constructed using the principles of conservation of mass, momentum, and total kinetic energy; the process has been described in detail in Ref. [31]. The mass resolution of the spectrometer was ± 2 u and the TKE resolution was ± 10 MeV.

III. RESULTS AND DISCUSSION

The measured mass-total kinetic energy distributions of the binary fragments formed in the three reactions ^{84}Kr $+$ ^{198}Pt, ^{86}Kr $+$ ^{198}Pt, and ^{86}Kr $+$ ^{197}Au at energies above the calculated Bass barrier are shown in Fig. 1. To take into account the angular distributions for both symmetric as well as asymmetric fragments, data in the laboratory angles 30° to 68° were integrated and normalized with respect to elastic events. It is observed that the majority of fragments are target and

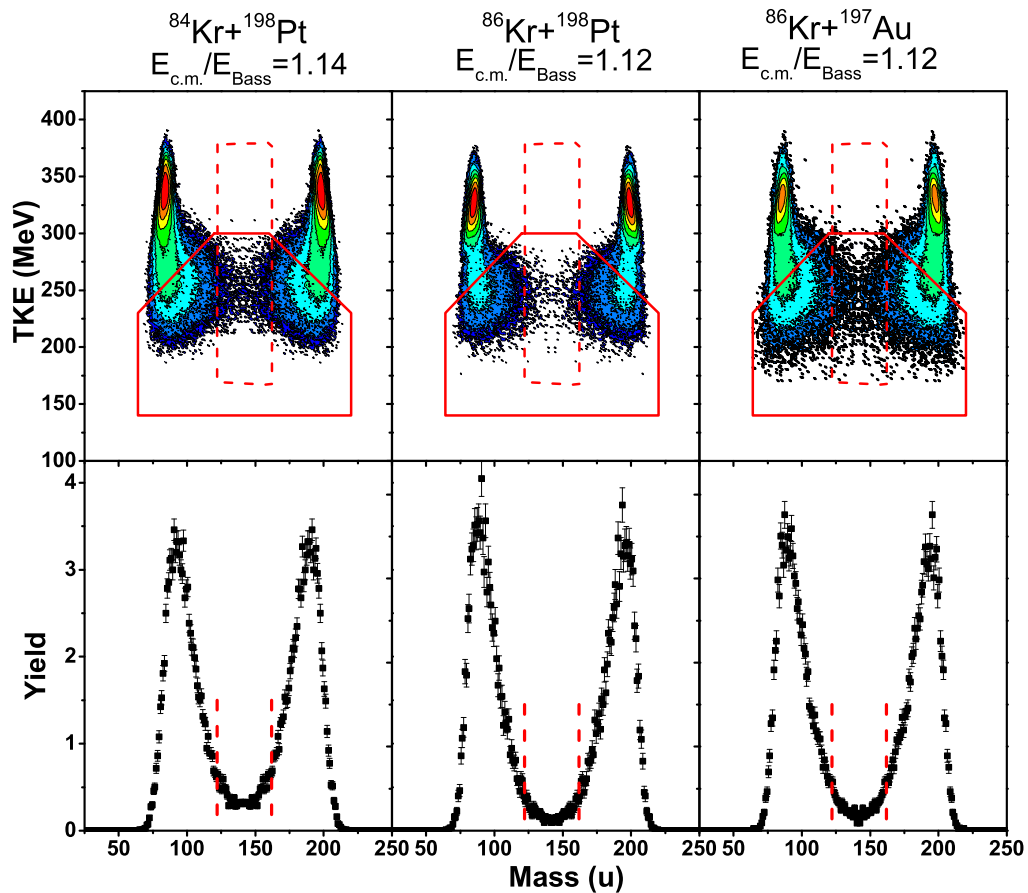FIG. 1. The M-TKE distributions of the binary fragments formed in the reactions ^{84}Kr + ^{198}Pt, ^{86}Kr + ^{198}Pt, and ^{86}Kr + ^{197}Au at the above barrier energies. The red continuous contour represents the events selected for analysis arising from capture. Lower panel represents the projections of mass yield under this continuous contours. The contours with the dashed lines represent the symmetric fragments with $A_{CN}/2 \pm 20$ u.

projectile like nuclei; they are identified as quasielastic and deep inelastic fragments. The fission like fragments located between the quasielastic/deep inelastic peaks are considered to be relaxed events, which are called *capture events*. The capture events can originate from either compound nuclear fission or quasifission processes. These events are marked by the red continuous contour lines in the M-TKE distributions in Fig. 1 (upper panels). The lower panels of Fig. 1 represent the projected mass distributions of the fragments under the contour. It is noted that for the reaction ^{84}Kr + ^{198}Pt, the relative contributions of the symmetric events are larger compared to the other two reactions.

It is known from earlier studies [25,26,28] that, for the systems with $\sim Z = 108$–114, the standard deviation of fission fragment mass distributions for compound nuclear fission is about 20 u. Therefore, to evaluate the compound nuclear fission like events, the fragments with masses $A_{CN}/2 \pm 20$ u are selected (by the dashed contour lines in Fig. 1) in the M-TKE distributions and they are called *symmetric fragments*.

In Fig. 2, we show the relative contributions of symmetric fragments in capture cross sections (i.e., the ratio of events inside the dashed and the solid contours of Fig. 1) and their variation with energy for the reactions ^{84}Kr + ^{198}Pt, ^{86}Kr + ^{198}Pt,

and ^{86}Kr + ^{197}Au. The data for the reaction ^{52}Cr + ^{232}Th [27], producing similar compound nucleus ($Z = 114$)
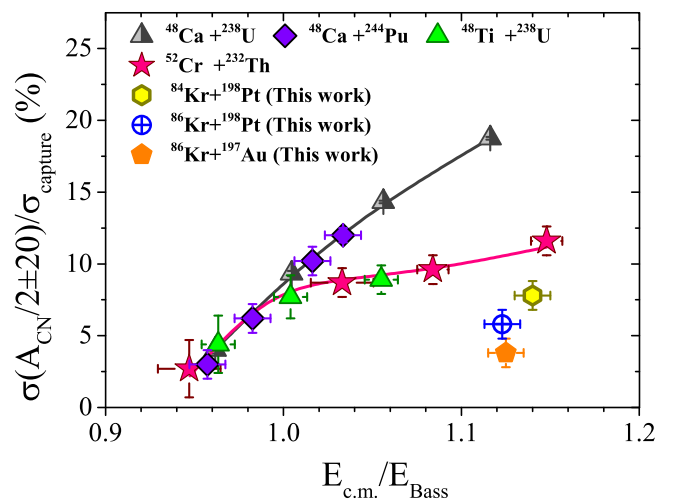

FIG. 2. Contributions of the symmetric fragments ($A_{CN}/2 \pm 20$ u) to the capture cross sections as a function of beam energy. The data for the ^{48}Ca, ^{48}Ti, and ^{52}Cr-induced reactions is from our earlier work [27].

as in the ^{86}Kr + ^{198}Pt reaction, as well as the data for the two extensively studied reactions ^{48}Ca + ^{244}Pu and ^{48}Ti + ^{238}U (producing $Z = 112$) are also presented for comparison. It is evident from Fig. 2 that for the three systems (^{84}Kr + ^{198}Pt, ^{86}Kr + ^{198}Pt, and ^{86}Kr + ^{197}Au) under the study in this work, the relative contributions of symmetric fragments in the capture events are much lower than those of similar reactions (^{48}Ca + ^{238}U, ^{244}Pu, or ^{52}Cr + ^{232}Th) with more asymmetric target projectile combinations and lower charge product Z_pZ_t. For the reactions with heavier ions like ^{84,86}Kr, the reactions are dominated by quasifission and thus the contributions of symmetric fission fragments are much lower. However, it is interesting to note that the dynamics involved in quasifission change even in the three target projectile combinations under study. At similar $E_{c.m.}/E_{Bass}$, the relative contributions of symmetric fragments in the total capture cross sections are different in the three reactions. The reaction ^{84}Kr + ^{198}Pt shows a significantly higher contribution of symmetric fragments than that of the reaction ^{86}Kr + ^{198}Pt. However, it is lower than that of ^{52}Cr + ^{232}Th reaction which populates a similar compound nucleus with $Z = 114$. Among the systems studied here, ^{86}Kr + ^{197}Au reaction that populates $Z = 115$, shows the lowest contribution of symmetric fragments in the capture cross sections.

Recent calculation [32] of the potential energy surface as a function of elongation and mass asymmetry for a heavy-ion-induced reaction indicates that in the fission of superheavy composite, the mass-symmetric fragments may be formed by different modes; they may originate either from CNF or from symmetric quasifission (symQF) process or even from the tail of asymmetric quasifission (asymQF) process. However, for the ^{84,86}Kr-induced reactions, so far as symmetric fragments are concerned, the contribution of CNF is negligible; and only the mechanism of quasifission prevails [33]. The measurement of TKE is useful in disentangling the contributions of symQF and asymQF. The TKE of CNF can be predicted by the Viola systematics. While the TKE of symQF is larger than that of CNF, it is lower in the case of asymQF [27].

The measured TKE distributions of the symmetric fragments (with $A_{CN}/2 \pm 20$ u) for all the three reactions are shown in Fig. 3. Following the procedure prescribed in Ref. [27], the TKE distributions have been fitted with two Gaussian distributions corresponding to symQF and asymQF. The lower energy component (green shade, right hashed) is attributed to the asymQF and the higher energy component (red shade, left hashed) arises from symQF. As it is expected that in such symmetric reactions under study, the presence of binary events originating from the compound nuclear process will be negligible, the two Gaussian distributions are sufficient to fit the TKE distributions. The peak of the asymmetric component was fixed from systematics [12] and the variance of the asymmetric part was set to the experimental value of the TKE for the maximum yield of the asymmetric quasifission [34]. The parameters for the symQF were estimated following the decomposition of the TKE distributions for the reaction ^{86}Kr + ^{198}Pt [27].

The Viola systematics [35] predicts the most probable value of the TKE distribution of the symmetric fragments fol-
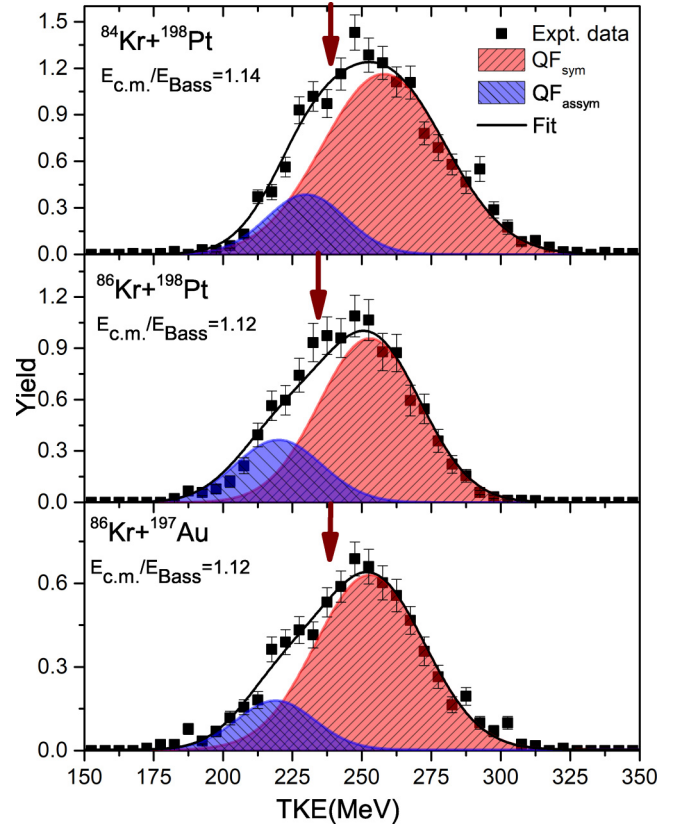

FIG. 3. TKE distributions of the symmetric fragments ($A_{CN}/2 \pm 20$ u), for the three reactions. The red shaded (left hashed) portion represents the estimation of symmetric quasifission, while the green portion (right hashed) represents the asymmetric quasifission. The blue (solid) line represents the overall fit. The arrow represents the kinetic energy as predicted by the Viola systematics for symmetric fragments.

lowing the formation of the compound nucleus. The deviation of average TKE from the Viola systematics for the symmetric fragments formed in the reactions ^{84}Kr + ^{198}Pt, ^{86}Kr + ^{198}Pt, and ^{86}Kr + ^{197}Au and their variation with beam energy are presented in Fig. 4. For all three systems, it is observed that the average total kinetic energy is higher than the respective prediction of the Viola systematics. The results for the reactions ^{48}Ca + ^{238}U, producing superheavy elements $Z = 112$ and ^{52}Cr + ^{232}Th that produce similar SHE with $Z = 114$ are also presented for comparison. It is interesting to note that for the reactions with asymmetric projectile target combinations, the average total kinetic energy is lower than the prediction of the Viola systematics due to the dominance of asymQF [26]. It is, however, argued [12] that in the case of symQF the average TKE should be higher compared to CN fission due to the strong influence of closed shells at $Z = 50$ and $N = 82$. The observation of higher values of average TKE compared to the Viola systematics thus also indicates that in the reactions ^{84}Kr + ^{198}Pt, ^{86}Kr + ^{198}Pt, and ^{86}Kr + ^{197}Au the major part of the symmetric fragments originates from the symQF process as is found in the analysis of TKE distributions as shown in Fig. 3.
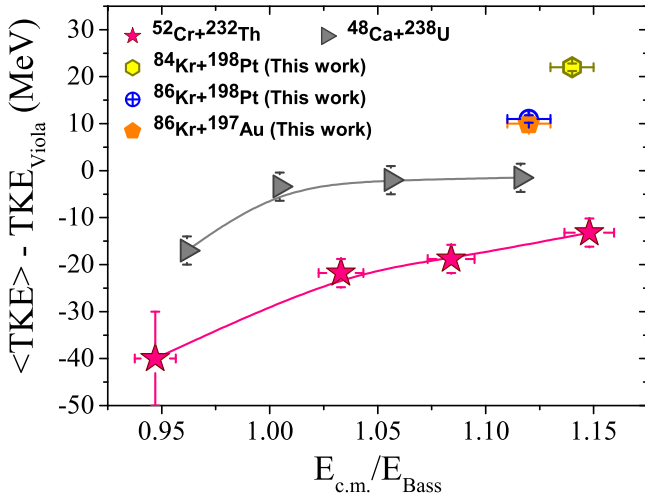
FIG. 4. The deviation of average TKE from the Viola systematics for the symmetric fragments, as a function of beam energy with respect to the calculated Bass barrier. The data for the ^{48}Ca- and ^{52}Cr-induced reactions is taken from Ref. [27].

As equilibration is not complete in the QF process, the dissipation of energy in QF is less than that of the fusion-fission process. The width of the TKE distribution is sensitive to the dissipation dynamics of a nuclear reaction. The standard deviations of TKE (σ_{TKE}) of the symmetric fragments with masses $A_{CN}/2 \pm 20$ u are shown in Fig. 5. It is observed that σ_{TKE} is wider for the reactions with relatively lighter projectiles (e.g., ^{52}Cr) compared to that of the heavier projectiles ^{84,86}Kr indicating less dissipation of energy for the latter case. It is interesting to note that for the production of similar SHE with $Z = 114$, the variances of TKE for ^{84,86}Kr $+ ^{198}$Pt are lower than those of the ^{52}Cr $+ ^{232}$Th reaction but the average TKEs are higher (as shown in Fig. 4). This indicates that
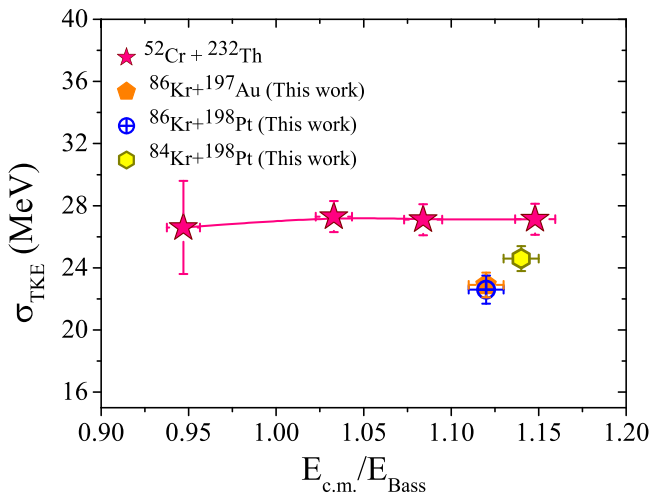

FIG. 5. The variation of the standard deviation of the total kinetic energy distributions with beam energy for the symmetric fragments with $A_{CN}/2 \pm 20$ u. The data for the ^{52}Cr-induced reaction are taken from our earlier work [27].
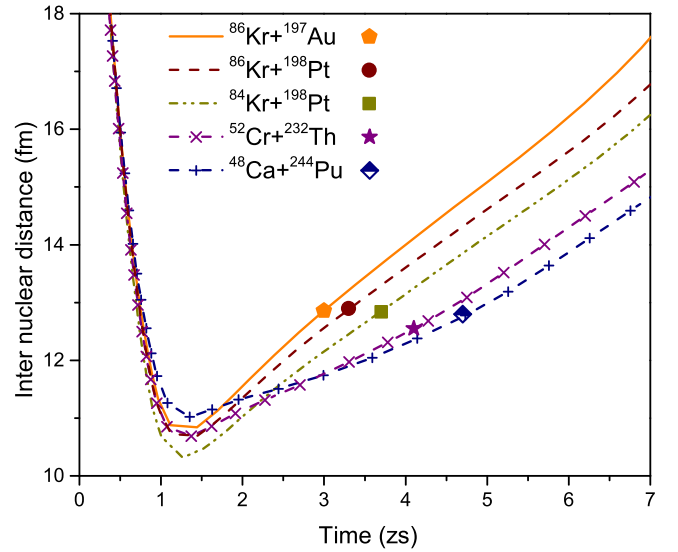

FIG. 6. Evolution of the internuclear distance of the dinucleus with time calculated using the dynamical code HICOL. The time taken for the dinuclear system to reach a size corresponding to the barrier radius (R_B) is shown by the symbols. The size of the symbols are larger than the uncertainty in the timescale.

krypton-induced reactions are dominated by symQF and interaction time is shorter.

The quasifission timescale has been observed [27] to depend on the target-projectile combination, with the timescale decreasing for more symmetric reactions. Using the relation between mean reaction time and mass drift proposed by Shen *et al.* [18], the mean quasifission time for asymmetric mass split was deduced to be ≈ 6.2 zs for ^{48}Ca $+ ^{244}$Pu, 4.8 zs for ^{52}Cr $+ ^{232}$Th, and 2.7 zs for ^{86}Kr $+ ^{198}$Pt [27]. Following the same prescription, the mean asymmetric quasifission time for the reactions ^{84}Kr $+ ^{198}$Pt, ^{86}Kr $+ ^{198}$Pt, and ^{86}Kr $+ ^{197}$Au studied in this work was found to be ≈ 3 zs. The accuracy of the mean quasifission time determined by this procedure is about 20% [36].

An analysis using the dynamical code HICOL [37] was carried out for the three systems under this study at the measured beam energies, along with two more reactions, ^{52}Cr $+ ^{232}$Th and ^{48}Ca $+ ^{244}$Pu, that populate nearby flerovium nuclei. The evolution of the internuclear distance of the dinuclear system with time has been studied as shown in Fig. 6. It is found that while ^{86}Kr $+ ^{197}$Au is the fastest evolving system, ^{48}Ca $+ ^{244}$Pu is the slowest. The time the dinuclear system took to reach a size corresponding to the barrier radius (R_B) [38] is marked in Fig. 6. The noted mean times were (3.0 $\pm$ 0.2) zs for ^{86}Kr $+ ^{197}$Au, (3.3 $\pm$ 0.2) zs for ^{86}Kr $+ ^{198}$Pt, (3.7 $\pm$ 0.2) zs for ^{84}Kr $+ ^{198}$Pt, (4.1 $\pm$ 0.2 zs) for ^{52}Cr $+ ^{232}$Th, and (4.7 $\pm$ 0.2) zs for ^{48}Ca $+ ^{244}$Pu. The uncertainties in time arise from the uncertainties in the nuclear radius. The trend that ^{48}Ca $+ ^{244}$Pu is the slowest to reach the radius R_B, while ^{86}Kr $+ ^{197}$Au is the fastest is also noted here. Compared to ^{86}Kr $+ ^{198}$Pt, the evolution of the reaction ^{84}Kr $+ ^{198}$Pt was found to be slower. The HICOL predicted time is similar to the value of the quasifission time that was deduced from
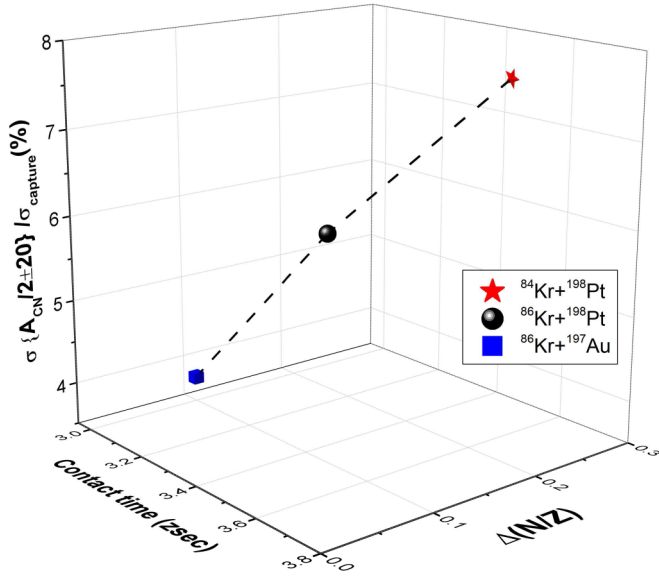
FIG. 7. Three-dimensional plot connecting the time predicted by HICOL for the dinucleus to reach a size corresponding to the barrier radius (R_B), with the entrance channel isospin difference, along with the relative yield of symmetric fragments for the three reactions.
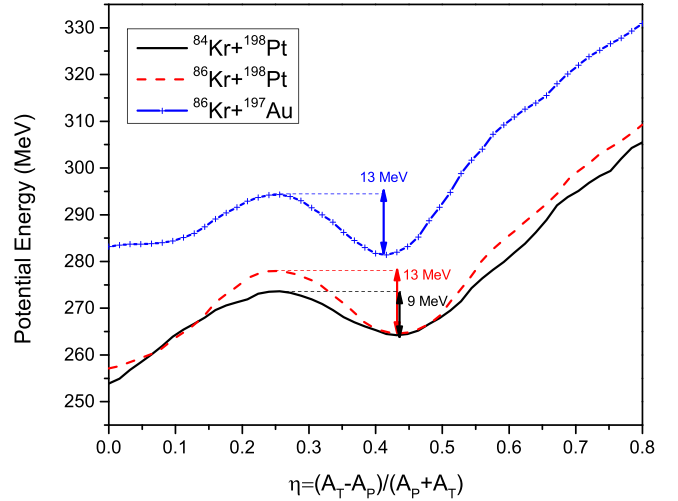

FIG. 8. Two-center shell-model calculation for the three systems studied in this work. The potential has been calculated for the mass asymmetry at the touching configuration of the target projectile combination. The arrows indicate the depth of the potential pocket.

the prescription of Shen *et al.* [18]. However, for the other two reactions, ^{52}Cr $+$ ^{232}Th and ^{48}Ca $+$ ^{244}Pu, the quasifission time (4.8 and 6.2 zs, respectively) calculated from Shen's prescription are slightly higher than that of the deduced (HICOL) time ($\approx$3.9 and 4.5 zs, respectively). As it is known that for the reactions ^{52}Cr $+$ ^{232}Th and ^{48}Ca $+$ ^{244}Pu the CN process has a finite probability of occurrence and it competes with the quasifission process, this extra time may be indicative of more equilibration in the dynamics for these systems.

The three quasifission-dominated reactions ^{86}Kr $+$ ^{197}Au, ^{86}Kr $+$ ^{198}Pt, and ^{84}Kr $+$ ^{198}Pt have entrance channel isospin difference $\Delta(N/Z) = 0.10$, 0.15, and 0.20, respectively. The entrance channel isospin difference is reported to play a role in the dynamics of the nuclear reaction [39]. In Fig. 7, we show a three-dimensional plot connecting the time predicted by HICOL for the dinucleus to reach a size corresponding to the barrier radius R_B (*x* axis), with the entrance channel isospin difference (*y* axis), along with the measured value of the relative yield of symmetric fragments (*z* axis) for the three reactions. It can be observed that the higher the entrance channel isospin difference, the more is the time taken by the dinucleus to reach the size of the barrier radius (R_B). The observation of more number of symmetric fragments in the capture cross sections for the ^{84}Kr $+$ ^{198}Pt reaction compared to ^{86}Kr $+$ ^{198}Pt also suggests that ^{84}Kr-induced reaction is relatively more equilibrated. This indicates the possible influence of the isospin degree of freedom in the quasifission dynamics. The present results reveal that the reactions with higher entrance channel isospin difference equilibrate slower than those with lower entrance channel isospin difference, thus driving the system toward more mass exchange and hence resulting in a more symmetric mass split. It is to be noted that the three reactions under study are quasifission dominated and can be considered as benchmark data in the dynamical

calculations of quasifission reactions with the isospin degree of freedom as a parameter.

The driving potential at the barrier radius (R_B) for the three systems are calculated using the two center shell-model potential at the ground state [40]. The depth of the pocket corresponding to asymmetric mass split has been quantified as shown in Fig. 8. It is found that the depth of the asymmetric pocket for the reaction ^{84}Kr $+$ ^{198}Pt is lower compared to the other two reactions ^{86}Kr $+$ ^{197}Au and ^{86}Kr $+$ ^{198}Pt. At finite temperatures, the depth of the pockets are expected to decrease, but it may be inferred that the relative depth of the pocket for ^{84}Kr $+$ ^{198}Pt will remain shallower compared to that for the other two reactions. This explains the higher yield of symmetric events as observed (shown in Fig. 2) for the reaction ^{84}Kr $+$ ^{198}Pt compared to the other two reactions studied in this work. For the calculation of potential, the entrance channel isospin difference was not considered as an explicit input; however, its influence may be present. An explicit theoretical calculation that includes the influence of the isospin difference in the entrance channel on the potential energy surface may further elucidate the phenomenon.

IV. SUMMARY

The mass-total kinetic energy distributions of fission like fragments formed in three reactions ^{84}Kr $+$ ^{198}Pt, ^{86}Kr $+$ ^{198}Pt, and ^{84}Kr $+$ ^{197}Au have been studied near the Coulomb barrier energies. It is observed that all three reactions have the characteristics of mass-total kinetic energy distributions dominated by the quasifission process. The total kinetic energy distributions could be explained by two components, arising from symmetric and asymmetric quasifission. For all reactions, the average total kinetic energy was found to be higher compared to the predictions of the Viola systematics indicating that the major part of the symmetric fragments originates from the symmetric quasifission process.

The standard deviations of total kinetic energy (σ_{TKE}) of the symmetric fragments were found to be narrower compared to the reactions with lighter projectiles (^{52}Cr) suggesting less dissipation of energy in the entrance channel for ^{84,86}Kr-induced reactions.

An analysis of the timescales of the reactions using HICOL shows that ^{84}Kr + ^{198}Pt takes a longer time to reach a particular dinuclear shape compared to the other two reactions, which may be due to the higher entrance channel isospin difference for this particular reaction. The driving potential at the barrier radius also shows a shallower pocket for ^{84}Kr + ^{198}Pt compared to that for ^{86}Kr + ^{198}Pt and ^{86}Kr + ^{197}Au reactions. It is found that the yield of binary fragments following symmetric quasifission is more for ^{84}Kr + ^{198}Pt compared to that of ^{86}Kr + ^{198}Pt reaction. This may be attributed to a possible change in the potential energy surface for the reaction ^{84}Kr + ^{198}Pt compared to ^{86}Kr + ^{198}Pt, due to the change in the entrance channel. An explicit dynamical calculation with the inclusion of the influence of the isospin difference in the entrance channel on the potential energy surface may further elucidate the phenomenon.

[1] Y. T. Oganessian, J. Phys. G **34**, R165 (2007).

[2] Y. T. Oganessian, V. K. Utyonkov, Y. V. Lobanov, F. S. Abdullin, A. N. Polyakov, I. V. Shirokovsky, Y. S. Tsyganov, G. G. Gulbekian, S. L. Bogomolov, B. N. Gikal, A. N. Mezentsev, S. Iliev, V. G. Subbotin, A. M. Sukhov, A. A. Voinov, G. V. Buklanov, K. Subotic, V. I. Zagrebaev, M. G. Itkis, J. B. Patin, K. J. Moody, J. F. Wild, M. A. Stoyer, N. J. Stoyer, D. A. Shaughnessy, J. M. Kenneally, P. A. Wilk, R. W. Lougheed, R. I. Il'kaev, and S. P. Vesnovskii, Phys. Rev. C **70**, 064609 (2004).

[3] Y. T. Oganessian, V. K. Utyonkov, Y. V. Lobanov, F. S. Abdullin, A. N. Polyakov, R. N. Sagaidak, I. V. Shirokovsky, Y. S. Tsyganov, A. A. Voinov, G. G. Gulbekian, S. L. Bogomolov, B. N. Gikal, A. N. Mezentsev, S. Iliev, V. G. Subbotin, A. M. Sukhov, K. Subotic, V. I. Zagrebaev, G. K. Vostokin, M. G. Itkis, K. J. Moody, J. B. Patin, D. A. Shaughnessy, M. A. Stoyer, N. J. Stoyer, P. A. Wilk, J. M. Kenneally, J. H. Landrum, J. F. Wild, and R. W. Lougheed, Phys. Rev. C **74**, 044602 (2006).

[4] Y. T. Oganessian, F. S. Abdullin, P. D. Bailey, D. E. Benker, M. E. Bennett, S. N. Dmitriev, J. G. Ezold, J. H. Hamilton, R. A. Henderson, M. G. Itkis, Y. V. Lobanov, A. N. Mezentsev, K. J. Moody, S. L. Nelson, A. N. Polyakov, C. E. Porter, A. V. Ramayya, F. D. Riley, J. B. Roberto, M. A. Ryabinin, K. P. Rykaczewski, R. N. Sagaidak, D. A. Shaughnessy, I. V. Shirokovsky, M. A. Stoyer, V. G. Subbotin, R. Sudowe, A. M. Sukhov, Y. S. Tsyganov, V. K. Utyonkov, A. A. Voinov, G. K. Vostokin, and P. A. Wilk, Phys. Rev. Lett. **104**, 142502 (2010).

[5] P. Moller and A. J. Sierk, Nature (Lond.) **422**, 485 (2003).

[6] B. B. Back, R. R. Betts, K. Cassidy, B. G. Glagola, J. E. Gindler, L. E. Glendenin, and B. D. Wilkins, Phys. Rev. Lett. **50**, 818 (1983)

[7] V. Zagrebaev and W. Greiner, J. Phys. G **34**, 1 (2007).

[8] D. J. Hinde, M. Dasgupta, and E. C. Simpson, Prog. Part. Nucl. Phys. **118**, 103856 (2021).

[9] E. Vardaci, M. G. Itkis, I. M. Itkis, G. Knyazheva, and E. M. Kozulin, J. Phys. G: Nucl. Part. Phys. **46**, 103002 (2019).

[10] A. N. Andreyev, K. Nishio, and K.-H. Schmidt, Rep. Prog. Phys. **81**, 016301 (2017).

[11] R. du Rietz, E. Williams, D. J. Hinde, M. Dasgupta, M. Evers, C. J. Lin, D. H. Luong, C. Simenel, and A. Wakhle, Phys. Rev. C **88**, 054618 (2013).

[12] M. G. Itkis, E. Vardaci, I. M. Itkis, G. N. Knyazheva, and E. M. Kozulin, Nucl. Phys. A **944**, 204 (2015).

[13] Y. Aritomo, K. Hagino, K. Nishio, and S. Chiba, Phys. Rev. C **85**, 044614 (2012).

[14] C. Simenel, Eur. Phys. J. A **48**, 152 (2012).

[15] G. G. Adamian, N. V. Antonenko, and W. Scheid, Nucl. Phys. A **678**, 24 (2000).

[16] A. K. Nasirov, G. Mandaglio, G. Giardina, A. Sobiczewski, and A. I. Muminov, Phys. Rev. C **84**, 044612 (2011).

[17] J. Toke, B. Bock, G. X. Dai, A. Gobbi, S. Gralla, K. D. Hildenbrand, J. Kuzminski, W. F. J. Müller, A. Olmi, and H. Stelzeret, Nucl. Phys. A **440**, 327 (1985).

[18] W. Q. Shen, J. Albinski, A. Gobbi, S. Gralla, K. D. Hildenbrand, N. Herrmann, J. Kuzminski, W. F. J. Müller, H. Stelzer, J. Toke, B. B. Back, S. Bjornholm, and S. P. Sorensen, Phys. Rev. C **36**, 115 (1987).

[19] J. P. Blocki, W. J. Swiatecki, and H. Feldmeier, Nucl. Phys. A **459**, 145 (1986)

[20] A. C. Berriman, D. J. Hinde, M. Dasgupta, C. R. Morton, R. D. Butt, and J. O. Newton, Nature (Lond.) **413**, 144 (2001).

[21] R. Tripathi, K. Sudarshan, S. Sodaye, A. V. R. Reddy, K. Mahata, and A. Goswami, Phys. Rev. C **71**, 044616 (2005).

[22] T. K. Ghosh, S. Pal, K. S. Golda, and P. Bhattacharya, Phys. Lett. B **627**, 26 (2005).

[23] A. Chaudhuri, A. Sen, T. K. Ghosh, K. Banerjee, Jhilam Sadhukhan, S. Bhattacharya, P. Roy, T. Roy, C. Bhattacharya, Md. A. Asgar, A. Dey, S. Kundu, S. Manna, J. K. Meena, G. Mukherjee, R. Pandey, T. K. Rana, V. Srivastava, R. Dubey, Gurpreet Kaur et al., Phys. Rev. C **94**, 024617 (2016).

[24] D. J. Hinde et al., EPJ Web Conf. **66**, 03037 (2014).

[25] E. M. Kozulin, G. N. Knyazheva, S. N. Dmitriev, I. M. Itkis, M. G. Itkis, T. A. Loktev, K. V. Novikov, A. N. Baranov, W. H. Trzaska, E. Vardaci, S. Heinz, O. Beliuskina, and S. V. Khlebnikov, Phys. Rev. C **89**, 014614 (2014).

[26] E. M. Kozulin, G. N. Knyazheva, K. V. Novikov, I. M. Itkis, M. G. Itkis, S. N. Dmitriev, Yu. Ts. Oganessian,

A. A. Bogachev, N. I. Kozulina, I. Harca, W. H. Trzaska, and T. K. Ghosh, Phys. Rev. C **94**, 054613 (2016).

[27] E. M. Kozulin, G. N. Knyazheva, T. K. Ghosh, A. Sen, I. M. Itkis, M. G. Itkis, K. V. Novikov, I. N. Diatlov, I. V. Pchelintsev, C. Bhattacharya, S. Bhattacharya, K. Banerjee, E. O. Saveleva, and I. V. Vorobiev, Phys. Rev. C **99**, 014616 (2019).

[28] G. N. Knyazheva, E. M. Kozulin, R. N. Sagaidak, A. Y. Chizhov, M. G. Itkis, N. A. Kondratiev, V. M. Voskressensky, A. M. Stefanini, B. R. Behera, L. Corradi, E. Fioretto, A. Gadea, A. Latina, S. Szilner, M. Trotta, S. Beghini, G. Montagnoli, F. Scarlassara, F. Haas, N. Rowley, P. R. S. Gomes, and A. Szanto de Toledo, Phys. Rev. C **75**, 064602 (2007).

[29] P. Moller *et al.*, Atom. Data Nucl. Data Tab. **59**, 185 (1995).

[30] M. G. Itkis *et al.*, Nucl. Phys. A **734**, 136 (2004).

[31] E. M. Kozulin *et al.*, Instrum. Exp. Tech. **51**, 44 (2008).

[32] V. I. Zagrebaev and W. Greiner, Nucl. Phys. A **944**, 257 (2015).

[33] M. G. Itkis *et al.*, Nucl. Phys. A **787**, 150 (2007).

[34] I. M. Itkis, E. M. Kozulin, M. G. Itkis, G. N. Knyazheva, A. A. Bogachev, E. V. Chernysheva, L. Krupa, Y. T. Oganessian, V. I. Zagrebaev, A. Y. Rusanov, F. Goennenwein, O. Dorvaux, L. Stuttge, F. Hanappe, E. Vardaci, and E. de Goes Brennand, Phys. Rev. C **83**, 064613 (2011).

[35] V. E. Viola, K. Kwiatkowski, and M. Walker, Phys. Rev. C **31**, 1550 (1985).

[36] G. N. Knyazheva, I. M. Itkis, and E. M. Kozulin, J. Phys.: Conf. Ser. **515**, 012009 (2014).

[37] H. Feldmeier, Rep. Prog. Phys. **50**, 915 (1987).

[38] R. Bass, *Nuclear Reactions with Heavy Ions* (Springer-Verlag, Berlin, 1980).

[39] C. Simenel *et al.*, Phys. Lett. B **710**, 607 (2012).

[40] V. I. Zagrebaev, A. S. Denikin, A. V. Karpov, A. P. Alekseev, M. A. Naumenko, V. A. Rachkov, V. V. Samarin, V. V. Saiko, A. Y. Kozin, NRV web knowledge base on low-energy nuclear physics, http://nrv.jinr.ru/nrv/.